

## Cross-Sectional Elasticity Imaging of Arterial Wall by Comparing Measured Change in Thickness with Model Waveform

Jiang TANG\*, Hideyuki HASEGAWA and Hiroshi KANAI

Graduate School of Engineering, Tohoku University, Sendai 980-8579, Japan

(Received November 12, 2004; accepted March 13, 2005; published June 24, 2005)

For the assessment of the elasticity of the arterial wall, we have developed the *phased tracking method* [H. Kanai *et al.*: IEEE Trans. Ultrason. Ferroelectr. Freq. Control **43** (1996) 791] for measuring the minute change in thickness due to heartbeats and the elasticity of the arterial wall with transcutaneous ultrasound. For various reasons, for example, an extremely small deformation of the wall, the minute change in wall thickness during one heartbeat is largely influenced by noise in these cases and the reliability of the elasticity distribution obtained from the maximum change in thickness deteriorates because the maximum value estimation is largely influenced by noise. To obtain a more reliable cross-sectional image of the elasticity of the arterial wall, in this paper, a matching method is proposed to evaluate the waveform of the measured change in wall thickness by comparing the measured waveform with a template waveform. The maximum deformation, which is used in the calculation of elasticity, was determined from the amplitude of the matched model waveform to reduce the influence of noise. The matched model waveform was obtained by minimizing the difference between the measured and template waveforms. Furthermore, a random error, which was obtained from the reproducibility among the heartbeats of the measured waveform, was considered useful for the evaluation of the reliability of the measured waveform. [DOI: 10.1143/JJAP.44.4588]

KEYWORDS: change in wall thickness, elasticity, matching, reliability

### 1. Introduction

Recently, the increasing number of patients suffering from myocardial infarction or cerebral infarction has become a serious social problem. Therefore, it is important to diagnose atherosclerosis at an early stage because such circulatory diseases are mainly caused by atherosclerosis. Since the elasticity of the arterial wall changes as atherosclerosis develops,<sup>1)</sup> the evaluation of the regional elasticity of the arterial wall using ultrasound is useful for the diagnosis of atherosclerosis. For the assessment of the elasticity of the arterial wall, we developed a method, the *phased tracking method*,<sup>2)</sup> of measuring the change of several tens of microns in wall thickness due to heartbeats with transcutaneous ultrasound.<sup>3–7)</sup> However, particularly in a hard region, the change in thickness becomes several microns, and the measurement of such a minute change in thickness may be influenced by noise. Although the elastic modulus of the wall is obtained from the maximum change in thickness, the maximum value estimation is easily influenced by noise. In this paper, by employing a model waveform of the change in wall thickness which is considered to be noise free, a matching method to evaluate the reliability of the elasticity image is proposed. The model waveform was fitted to the measured waveform using the least-squares method to obtain the matched model waveform. The maximum deformation of the wall was obtained from the amplitude of the matched model waveform to reduce the influence of noise. Furthermore, the reproducibility among heartbeats of the measured waveform will be useful for the evaluation of the reliability.

### 2. Principles

#### 2.1 Elasticity estimation

An ultrasonic beam was sequentially scanned at 60 positions with a linear-type ultrasonic probe of 7.5 MHz using conventional ultrasound diagnostic equipment (Toshiba SSH-140A), and multiple ( $N_m + 1$ ) points were

preset from the luminal surface to the adventitia along the  $m$ th ultrasonic beam ( $m = 1, \dots, 60$ ) with constant intervals of  $h_0 = 375 \mu\text{m}$  at time  $t_0$  just before the ejection period. By dividing the arterial wall into multiple layers, we defined the  $n$ th layer ( $n = 1, \dots, N_m$ ) as being between two contiguous points,  $n$  and  $n + 1$ , along each beam. For the measurement of the change in the thickness of each of the  $N_m$  layers, the instantaneous depth  $x_{m,n}(t)$  of the  $n$ th point along the  $m$ th beam was simultaneously tracked by applying the *phased tracking method*<sup>2)</sup> to the received ultrasound. The minute decrease of several tens of a micrometer in the thickness of the  $n$ th layer resulting from the arrival of a pressure wave at the beginning of the ejection period was determined using  $\Delta h_{m,n}(t) = x_{m,n+1}(t) - x_{m,n}(t) - h_0$ .

From the ratio of the maximum decrease in thickness during one heartbeat,  $\Delta h_{m,n,\text{max}} = \max_t |\Delta h_{m,n}(t)|$ , to the initial thickness  $h_0$  of the  $n$ th layer, the maximum deformation of the  $n$ th layer was obtained using  $\Delta \varepsilon_{m,n,\text{max}} = \Delta h_{m,n,\text{max}}/h_0$ . Because the deformation was sufficiently small and was in the linear regime, it showed an incremental strain in the radial direction. By assuming that the arterial wall is incompressible and that the blood pressure is applied perpendicular to each layer, the elastic modulus of the  $n$ th layer along the  $m$ th beam,  $E_{\theta,m,n}$ , is approximately given by<sup>8)</sup>

$$E_{\theta,m,n} \cong \frac{1}{2} \left( \frac{\rho_{m,n,0}}{h_0 \cdot N_m} + \frac{N_m - n + 1}{N_m} \right) \frac{\Delta p}{\Delta \varepsilon_{m,n,\text{max}}} \quad (n = 1, \dots, N_m; m = 1, \dots, M), \quad (2.1)$$

where  $\rho_{m,n,0}$  is the initial inner radius of curvature of the  $n$ th layer along the  $m$ th beam at time  $t_0$ . We assumed that the pressure in the arterial wall decreases linearly with the distance from the intimal side to the adventitia and that the arterial wall is almost isotropic.<sup>9)</sup>

For the region with a length of 18 mm along the axis of the artery, the regional elasticity  $E_{\theta,m,n}$  was estimated on the cross-sectional image. Because the reflected ultrasound was received at a sampling interval of 100 ns (= 75  $\mu\text{m}$  along depth direction) after the quadrature demodulation, we

\*E-mail address: hkanai@ecei.tohoku.ac.jp

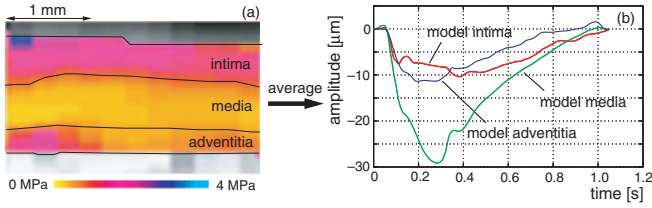


Fig. 1. Preparation of model waveforms. (a) Regions assigned as intima, media, and adventitia in elasticity image showing typical layered structure. (b) Model waveforms obtained by averaging changes in thickness in respective assigned regions.

further divided each layer with a thickness of  $h_0$  into 5 points, shifted the initial depth of each layer by one fifth of  $h_0$ , and applied the above procedure to each depth. Thus,  $E_{\theta,m,n}$  was estimated at intervals of  $75\mu\text{m}$  in the depth direction and  $300\mu\text{m}$  in the axial direction. Using a silicone rubber tube with two layers set in an artificial circulation system,<sup>8)</sup> the accuracy of the measurement of the regional elasticity of each layer has already been validated to be  $\approx 0.1\text{MPa}$ <sup>8)</sup>—that is, the error is  $\approx 8\%$  of the elasticity obtained by a separate static pressure-diameter test.

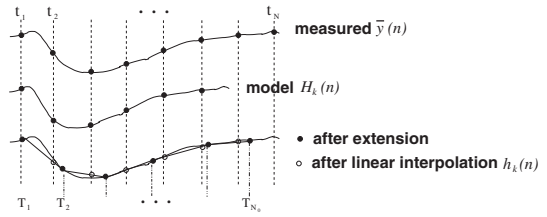


Fig. 2. Linear interpolation.

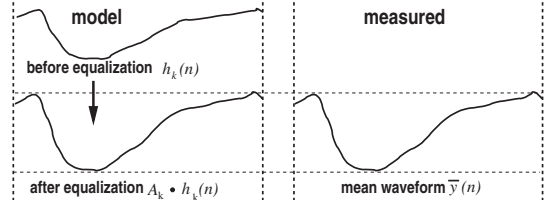


Fig. 3. Amplitude equalization.

### 2.2 Matching process

In our matching process, template waveforms were prepared as model waveforms,  $H_k(n)$  ( $n = 1, 2, \dots, N_0$ ), of

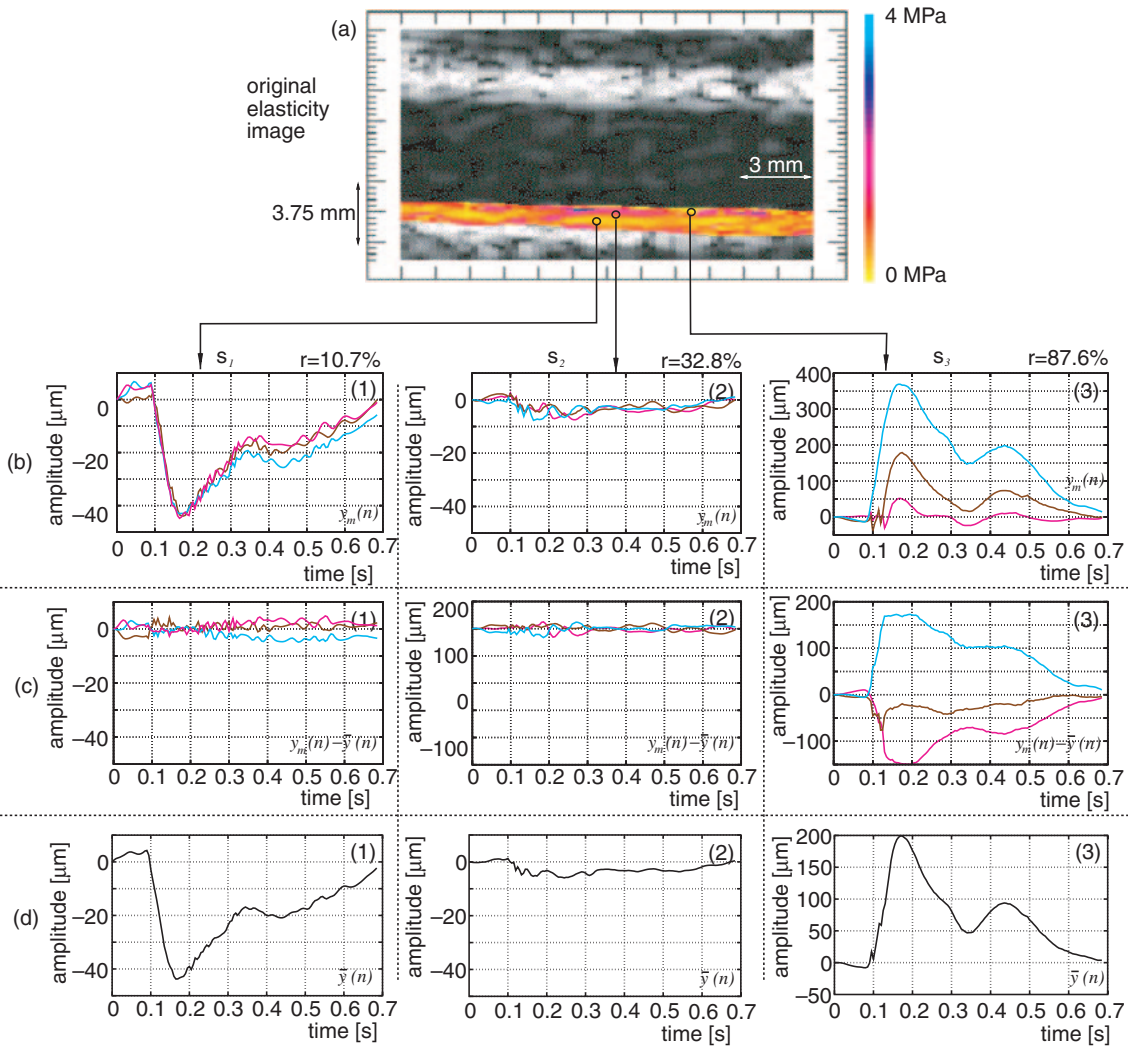


Fig. 4. *In vivo* measurement of mean waveform of changes in thickness of human carotid artery of 32-year-old subject. (a) Elasticity image obtained from maximum change in wall thickness. (b) Measured change in thickness waveform,  $y_m(n)$ , for each heartbeat. (c) Differences,  $y_m(n) - \bar{y}(n)$ , between mean waveform and measured waveforms,  $y_m(n)$ . (d) Measured mean waveform,  $\bar{y}(n)$ .

the change in wall thickness. A model waveform is fitted to the measured waveform as follows: A model waveform,  $H_k(n)$ , is fitted to a mean waveform,  $\bar{y}(n)$  ( $n = 1, 2, \dots, N$ ), of changes in thickness,  $y_m(n)$  ( $m = 1, 2, \dots, M$ ;  $n = 1, 2, \dots, N_m$ ), measured for  $M$  heartbeats. The mean waveform,  $\bar{y}(n)$ , is obtained using

$$\bar{y}(n) = \frac{1}{M} \sum_{m=1}^M y_m(n) \quad (n = 1, 2, \dots, N), \quad (2.2)$$

where the least number of sampled points in a heart cycle among  $M$  heartbeats is used for the number of sampled points  $N$  of the mean waveform.

In this paper, three types of model waveform,  $H_k(n)$  ( $k = 1, 2, 3$ ), were prepared for the intima, media, and adventitia regions because mechanical properties of these layers are different from each other.<sup>10)</sup> In a measured data showing a typical layered structure in the elasticity image, three layers were manually assigned, as shown in Fig. 1(a). As shown in Fig. 1(b), three model waveforms for the intima, media, and adventitia regions were obtained by averaging changes in thickness within the respective assigned regions.

Since the cardiac cycle differs among the subjects and the sampling frequency differs among the types of equipments used, the number of sampled points, which is related to the change in thickness waveform for one heart cycle, also differs. Therefore, as shown in Fig. 2, the model waveform,  $H_k(n)$ , was expanded or compressed to the same time length as the measured mean waveform,  $\bar{y}(n)$ , in the time axis, and then, linearly interpolated. The model waveform after interpolation,  $h_k(n)$  ( $n = 1, 2, \dots, N$ ), can be determined using

$$h_k(n) = H_k(n-1) + \frac{H_k(n) - H_k(n-1)}{T_n - T_{n-1}} \cdot (t_n - T_{n-1})$$

$$(n = 2, 3, \dots, N; h_k(1) = H_k(1)), \quad (2.3)$$

where  $t_n$  and  $T_n$  are the times at the  $n$ th point after and before linear interpolation.

Then, as shown in Fig. 3, the amplitude of the interpolated model waveform,  $h_k(n)$ , is equalized to the measured mean waveform,  $\bar{y}(n)$ , by minimizing the root mean squared difference,  $\alpha_k$ , between the model waveform,  $h_k(n)$ , and the measured waveform,  $\bar{y}(n)$ , using

$$\alpha_k = \sqrt{\sum_{n=1}^N |A_k h_k(n) - \bar{y}(n)|^2}, \quad (2.4)$$

where  $A_k$  is a constant that expresses the difference in amplitude between the measured and model waveforms. To determine the constant  $\hat{A}_k$  that minimizes  $\alpha_k$ , the partial derivative of  $\alpha_k$  with respect to  $A_k$  is set to zero.

$$\frac{\partial \alpha_k^2}{\partial A_k} = \frac{\partial}{\partial A_k} \left( \sum_{n=1}^N |A_k h_k(n) - \bar{y}(n)|^2 \right) = 0. \quad (2.5)$$

Equation (2.5) is rewritten as

$$2A_k \sum_{n=1}^N \{h_k(n)\}^2 - 2 \sum_{n=1}^N h_k(n) \bar{y}(n) = 0. \quad (2.6)$$

Then, the constant  $\hat{A}_k$  that minimizes  $\alpha_k$  is determined using

$$\hat{A}_k = \frac{\sum_{n=1}^N h_k(n) \cdot \bar{y}(n)}{\sum_{n=1}^N |h_k(n)|^2}. \quad (2.7)$$

The constant  $\hat{A}_k$  determined by eq. (2.7) is substituted into eq. (2.4) to calculate the residual difference  $\alpha_{k,\min}$ , which shows the difference between the measured and model waveforms expressed as

$$\alpha_{k,\min} = \sqrt{\sum_{n=1}^N |\bar{y}(n)|^2 - \frac{\left| \sum_{n=1}^N h_k(n) \bar{y}(n) \right|^2}{\sum_{n=1}^N |h_k(n)|^2}}. \quad (2.8)$$

The bias error  $b_k$  is defined as

$$b_k = \frac{\alpha_{k,\min}}{\sqrt{\sum_{n=1}^N |\bar{y}(n)|^2}} = \sqrt{1 - \frac{\left| \sum_{n=1}^N h_k(n) \bar{y}(n) \right|^2}{\sum_{n=1}^N |h_k(n)|^2 \cdot \sum_{n=1}^N |\bar{y}(n)|^2}}. \quad (2.9)$$

The amplitude of the model waveform,  $h_k(n)$ , is preset so as to give an elastic modulus  $E_\theta^h$  of 1 MPa. The elastic modulus  $E_{\theta,m,n}$  is determined using one of the estimated constants,  $\hat{A}_k$ , with the least bias error using

$$E_\theta^h = \frac{1}{\hat{A}_k} \quad [\text{MPa}]. \quad (2.10)$$

Furthermore, the normalized random error  $r$  between the mean waveform  $\bar{y}(n)$  and the measured waveforms  $y_m(n)$  of  $M$  heartbeats is defined as

$$r = \sqrt{\frac{\frac{1}{N} \sum_{n=1}^N \left( \frac{1}{M} \sum_{m=1}^M |y_m(n) - \bar{y}(n)|^2 \right)}{\frac{1}{N} \sum_{n=1}^N |\bar{y}(n)|^2}}. \quad (2.11)$$

$r$  shows the average amplitude of random errors during  $M$  cardiac cycles.

### 3. In vivo Experiments

Figures 4 and 5 show the measurement of the mean change in thickness waveforms and the matching process for a 32-year-old male subject, respectively. Figure 4(a) shows the cross-sectional elasticity image of the carotid arterial wall obtained from the maximum change in thickness. In systole, the artery diameter is expanded by an increase in internal pressure, and the wall thickness becomes smaller as shown by the measured mean waveforms  $\bar{y}(n)$  in the regions

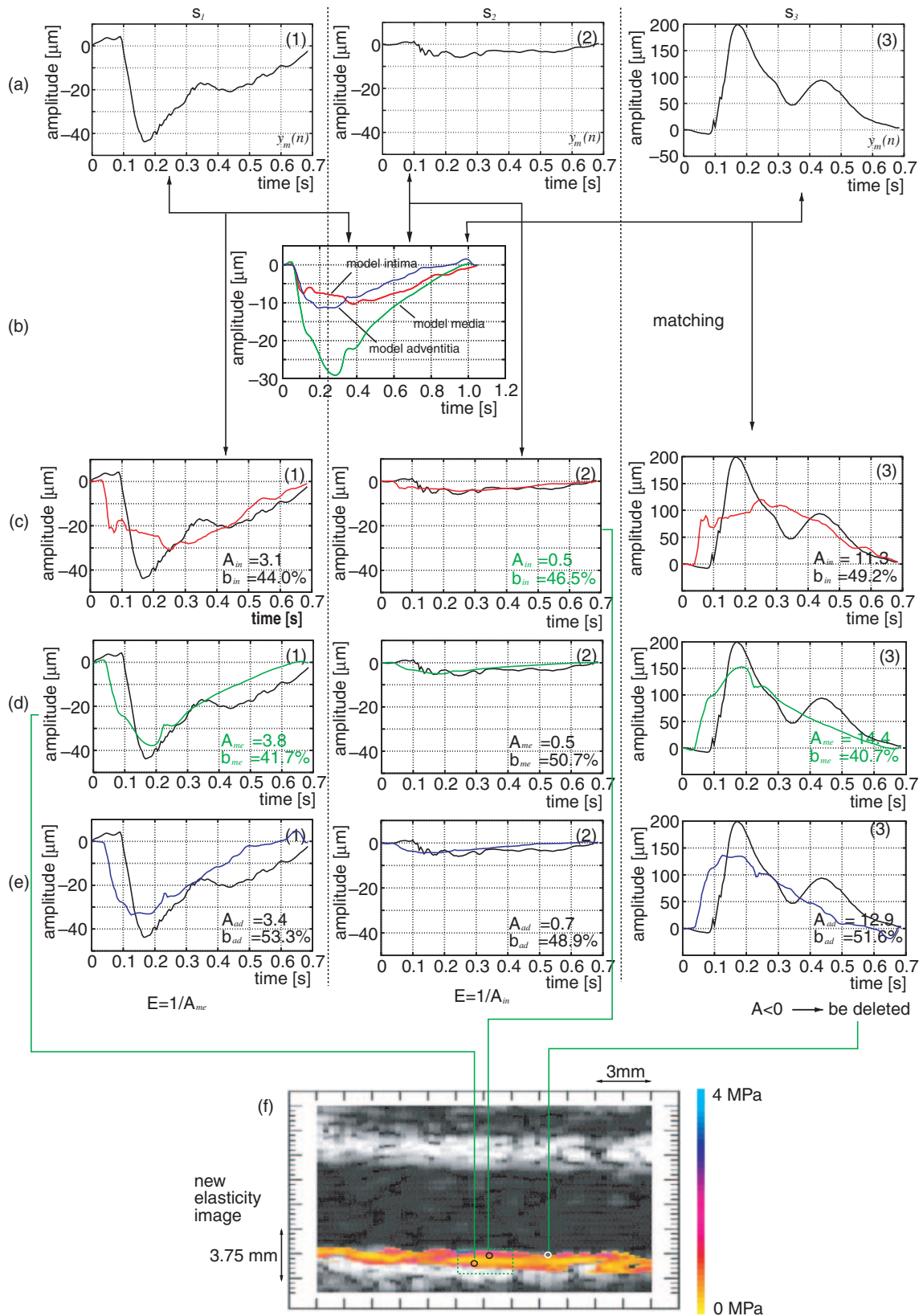


Fig. 5. Matching process using three model waveforms for 32-year-old subject. (a) Measured mean waveform,  $\bar{y}_m(n)$ . (b) Model waveforms,  $H_k(n)$ . (c) Measured mean waveform,  $\bar{y}_m(n)$ , and matched model for intima region,  $h_1(n)$ . (d) Measured mean waveform,  $\bar{y}_m(n)$ , and matched model for media region,  $h_2(n)$ . (e) Measured mean waveform,  $\bar{y}_m(n)$ , and matched model for adventitia region,  $h_3(n)$ . (f) Elasticity image obtained from estimated constant,  $\hat{A}_k$ , with least bias error.

$s_1$  and  $s_2$  in Figs. 4(d-1) and 4(d-2) obtained from the waveform of each beat,  $y_m(n)$ , shown in Fig. 4(b). In such cases, the estimated constant  $\hat{A}_k$  for matching the model waveform  $h_k(n)$  to the measured one is positive as shown in

Figs. 5(c), 5(d), and 5(e). The elasticity of such a region was calculated using the estimated constant  $\hat{A}_k$  for the model that gives the least bias error. Figures 4(d) and 5(a) show the same measured mean waveform  $\bar{y}_m(n)$ . In the region  $s_3$  in

Fig. 4(a), the measured waveform shows an increase in wall thickness, as shown in Fig. 5(a-3). In such a region, the change in wall thickness is considered not to be measured successfully. The reason for such a region showing an increase in the wall thickness can be explained as follows: A change in wall thickness is obtained from the difference between displacements at two points along an ultrasonic beam. When this set of two points very closely approaches to the lumen, the point on the luminal side is located in the lumen. Because ultrasonic beams are set to be perpendicular to the wall, these beams are also perpendicular to the direction of blood flow. Therefore, the velocity detected in the lumen becomes zero or, if detected, becomes small and random because echoes cannot be obtained from the same blood particle due to blood flow and the particle cannot be tracked during an entire heart cycle. Thus, the time integral of velocity (= displacement) at the point on the luminal side becomes almost zero. On the other hand, the displacement at another point in the posterior wall is positive (the distance between the ultrasonic probe and the posterior wall increases). Therefore, the change in thickness obtained by subtracting the displacement at the luminal point from that at the point in the posterior wall becomes positive (showing an increase in thickness). In such cases, the estimated constant  $\hat{A}_k$  for each matched model is negative, as shown in Figs. 5(c-3), 5(d-3), and 5(e-3). Therefore, the elasticity in such a region was not displayed. Furthermore, the random error  $r$  was obtained from the difference  $y_m(n) - \hat{y}(n)$  shown in Fig. 4(c). Random errors are described at the top of Fig. 4(b).

Figure 5(f) shows the elasticity image obtained from the estimated constant  $\hat{A}_k$  with the least bias error. In Fig. 5(f), the elasticity is color-coded only when the constant  $\hat{A}_k$  is larger than zero.

#### 4. Discussion

In Fig. 6, bias error is plotted as a function of the distance from the lumen along each ultrasonic beam in the region surrounded by a green dashed line in Fig. 5(f). Figure 6(a) shows bias errors obtained using only one model waveform for the media region. Figure 6(b) shows the least bias error obtained using three model waveforms for the intima, media, and adventitia regions. In this study, three model waveforms were prepared because the mechanical properties of the intima, media, and adventitia are different. Using these three types of model, the bias error, which shows the difference between the model and measured waveforms, can be reduced as shown in Fig. 6. However, in this paper, we do not consider differences between a healthy subject and a patient. Further investigation is necessary to optimize the model waveforms.

The main purpose of this study is to evaluate the measured elasticity image on the basis of the measured waveform of the change in wall thickness. In this study, a region showing an increase in wall thickness in systole was rejected not to be displayed in an elasticity image because such a change in wall thickness is not reliable. In our future work, bias and random errors should be used for evaluating the reliability of a measured elasticity image quantitatively.

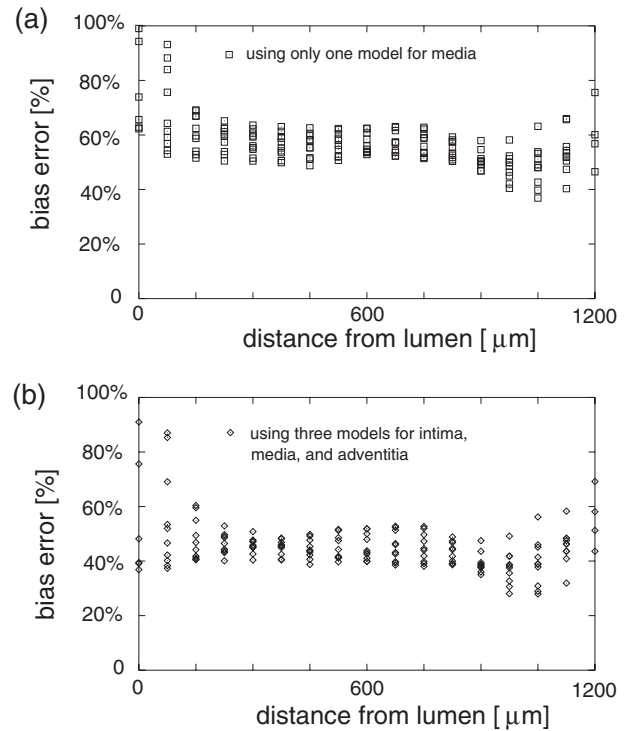


Fig. 6. Bias error distribution in region surrounded by green dashed line in Fig. 5(f). (a) Case of using only one model for media. (b) Case of using three models for intima, media, and adventitia.

#### 5. Conclusions

In this paper, a method for evaluating the reliability of the elasticity image by calculating the error between the measured and model waveforms of the change in wall thickness is proposed. Using the proposed method, a region showing an increase in wall thickness in systole (considered not to be reliable) was automatically rejected not to be displayed in an elasticity image. Further investigation is necessary to utilize bias and random errors for the quantitative evaluation of a measured elasticity image.

- 1) R. T. Lee, A. J. Grodzinsky, E. H. Frank, R. D. Kamm and F. J. Schoen: *Circulation* **83** (1991) 1764.
- 2) H. Kanai, M. Sato, Y. Koiwa and N. Chubachi: *IEEE Trans. UFFC* **43** (1996) 791.
- 3) H. Kanai, H. Hasegawa, N. Chubachi, Y. Koiwa and M. Tanaka: *IEEE Trans. UFFC* **44** (1997) 752.
- 4) H. Kanai, K. Sugimura, Y. Koiwa and Y. Tsukahara: *Electron. Lett.* **35** (1999) 949.
- 5) H. Kanai, Y. Koiwa and J. Zhang: *IEEE Trans. UFFC* **46** (1999) 1229.
- 6) H. Hasegawa, H. Kanai, N. Hoshimiya and Y. Koiwa: *Jpn. J. Med. Ultrason.* **31** (2004) 81.
- 7) H. Kanai, H. Hasegawa, M. Ichiki, F. Tezuka and Y. Koiwa: *Circulation* **107** (2003) 3018.
- 8) H. Hasegawa, H. Kanai, N. Hoshimiya and Y. Koiwa: *2000 IEEE Ultrason. Symp. Proc.* (2000) p. 1829.
- 9) D. J. Patel, J. S. Janicki, R. N. Vaishnav and J. T. Young: *Circ. Res.* **32** (1973) 93.
- 10) The Japan Society of Mechanical Engineers: *Mechanical Engineers' Handbook, Engineering, C6 Biotechnology and Medical Engineering*, Maruzen, Tokyo (1988) p. 147 [in Japanese].